PCCP

PAPER

View Article Online
View Journal | View Issue

Cite this: *Phys. Chem. Chem. Phys.*, 2020, **22**, 14637

Interference of a resonance state with itself: a route to control its dynamical behaviour

A. García-Vela

Received 23rd January 2020,
Accepted 5th June 2020

DOI: 10.1039/d0cp00392a

rsc.li/pccp

It is demonstrated both numerically and mathematically that the dynamical behavior of an isolated resonance state, which comprises the resonance decay lifetime and the asymptotic fragment state distribution produced upon resonance decay, can be extensively controlled by means of quantum interference induced by a laser field in the weak-field regime. The control scheme applied is designed to induce interference between amplitudes excited at two different energies of the resonance line shape, namely the resonance energy and an additional energy. This scheme exploits the resonance property of possessing a nonzero energy width, which makes it possible that a resonance state may interfere with itself, and thus allows interference between the amplitudes excited at the two energies of the resonance width. The application of this scheme opens the possibility of a universal control of both the duration and the fragment product distribution outcome of any resonance-mediated molecular process.

1 Introduction

Control of molecular processes is a goal that has been actively pursued in the last few decades. A variety of control strategies have been designed and applied, under both strong-field and weak-field (one-photon) conditions.[1–19] Strong-field control has been successful in achieving control targets in many molecular processes.[6,10,17] The possible disadvantage is that strong fields may produce undesired multiphoton ionization leading to the fragmentation of the molecular system. On the other hand, nondestructive weak-field control is typically based on quantum interference processes,[1,2,5,8,9,12,14,15] which, when properly applied, may lead to effects which are in practice very similar to those achieved with strong fields. Thus, pursuing the design of practical weak-field control schemes, albeit challenging, is of great interest.

A variety of molecular processes (among them photodissociation and reactive and non-reactive collisional processes) are governed by resonance states (either isolated or overlapping ones).[20–34] A strategy used to control those processes under weak-field conditions has been to modify the decay behaviour of the resonances involved by inducing quantum interference between them. In this sense, inducing interference between overlapping resonances excited within a superposition state has been successfully used to delay significantly radiationless transitions and intramolecular vibrational redistribution processes in different molecules.[21,23] Vibrational cooling was achieved by inducing resonance coalescence with a laser field.[26] Also in a framework of overlapping resonances, it has been shown that by means of interference between the resonances, it is possible to strongly enhance the lifetime of individual resonances within a superposition,[14,15,35,36] as well as to modify the fragment state distribution produced upon resonance decay.[30,36,37] Control over the resonance decay lifetime and over the fragment distribution provides control over both, the duration and the outcome, respectively, of the resonance-mediated molecular process of interest. In this latter case the control scheme applied was a simple but efficient one using a laser field that consisted of two pulses delayed in time, each pulse exciting a different energy at which several resonances overlap. Excitation of the two different energies is what induces interference between the overlapping resonances.

The possibility of modifying a resonance decay behaviour through interference between overlapping resonances has been thus widely demonstrated, and it allows for control of resonance-mediated molecular processes where such overlapping resonances are present. In addition to the processes mediated by overlapping resonances there are, however, other molecular processes mediated by isolated resonance states. The question thus arises whether it is possible to design similar control schemes that can be applied to these isolated-resonance processes. If so, control of resonance-mediated molecular processes would become universal, for any molecular system featuring either isolated or overlapping resonances. To the best of the author knowledge, such a control over isolated resonances has not yet been demonstrated.

Resonance states are intriguing quantum objects with very interesting properties. A well-known property of a resonance

Instituto de Física Fundamental, Consejo Superior de Investigaciones Científicas, Serrano 123, 28006 Madrid, Spain. E-mail: garciavela@iff.csic.es

state is that it possesses a nonzero energy width. Such a property makes it possible that an isolated resonance state can interfere with itself, which can be exploited in order to modify its decay behaviour, similar to that performed with overlapping resonances. In this work it is shown numerically and demonstrated formally that interference of an isolated resonance state with itself can be induced by applying a laser field. By controlling this interference, both the resonance lifetime and the asymptotic fragment state distribution produced upon resonance decay can be modified, allowing the control of any (isolated) resonance-mediated molecular process of interest.

2 Methodology

Any molecular process mediated by an isolated resonance state might be chosen to illustrate how the present control scheme works, and vibrational predissociation of the Ne–Br_2(B) complex is the specific choice in this study. This system features different types of resonances, and due to its relatively small size it can be described quantum mechanically, which is required to treat interference phenomena appropriately, and for this reason it is used in this study as a prototype system. Upon laser excitation, Ne–$Br_2(X,v'' = 0) + h\nu \rightarrow$ Ne–$Br_2(B,v',n')$, an intermolecular van der Waals resonance n' of Ne–$Br_2(B,v')$ is populated. The labels v'' and v' denote the vibrational states of Br_2 in the X and B electronic states, respectively, while n' labels the energy position of the resonance, with $n' = 0$ corresponding to the ground one. The resonance excited decays to the fragmentation continuum through vibrational predissociation, Ne–$Br_2(B,v',n') \rightarrow$ Ne + $Br_2(B,v_f < v')$. This process has been studied in detail both experimentally[38,39] and theoretically.[40,41]

Laser field excitation of Ne–$Br_2(B,v',n')$ and the subsequent predissociation was simulated with a full three-dimensional wave packet method described in detail elsewhere.[14,40] A Chebychev propagator, which is both accurate and efficient for the present purposes, was used. In order to assess the quality of the model applied, it is noted that the lifetime calculated with the present theoretical model for the decay of the -$Br_2(B,v' = 16)$ ground intermolecular resonance has been found to be 69 ps,[42] while the corresponding lifetime estimated experimentally is 68 ± 3 ps.[39] This good agreement with the experimental lifetime implies that both the three-dimensional wave packet method and the potential surfaces used in the present simulations are realistic enough in order to describe this resonance decay process.

In the simulations the wave packet is represented in Jacobian coordinates (R,r,θ), where R is the distance between the Ne atom and the Br_2 center of mass, r is the Br–Br internuclear distance, and θ is the angle between the vectors associated with R and r. In this representation the rovibrational eigenstates associated with the $Br_2(B,v,j)$ fragment are $\chi_v^{(j)}(r)P_j(\cos\theta)$, where $\chi_v^{(j)}(r)$ is the vibrational eigenfunctions of $Br_2(B)$ with associated energies $E_{v,j}$ and $P_j(\cos\theta)$ is a Legendre polynomial, with v and j being the Br_2 vibrational and rotational quantum numbers, respectively. The energy-resolved $Br_2(B,v,j)$ fragment state population is computed along time by projecting out the wave packet onto the corresponding states

$$P_{v,j}(E,t) = Ck_{v,j}\left|\int_0^t \left\langle \chi_v^{(j)}(r)P_j(\cos\theta)|\Phi(R_c,r,\theta,t')\right\rangle e^{iEt'/\hbar}dt'\right|^2, \quad (1)$$

where C is a constant factor, R_c is a suitably large distance of the dissociation coordinate R, E is the total energy of the system (which in the present simulations corresponds to the resonance energy $E = E_a$), and $k_{v,j}$ is given by

$$k_{v,j} = [2\mu(E - E_{v,j})]^{1/2}, \quad (2)$$

with μ being the Ne–Br_2 reduced mass. The population in each vibrational state of $Br_2(B,v)$ is now calculated as

$$P_v(E,t) = \sum_j P_{v,j}(E,t). \quad (3)$$

3 Results and discussion

Specifically, the simulations focus on the excitation of the Ne–$Br_2(B,v' = 21,n' = 4)$ intermolecular resonance ($n' = 4$ meaning the fourth excited resonance). The excitation spectrum associated with this resonance is shown in Fig. 1. This profile displays the Lorentzian shape characteristic of an isolated resonance state. The peak of the spectrum is located at the resonance energy $E = -38.90$ cm^{-1}, and its full width at half maximum is about FWHM = 0.4 cm^{-1}.

The goal is to modify the decay behaviour of the Ne–$Br_2(B,v' = 21,n' = 4)$ resonance, that is, its decay lifetime and the energy-resolved (at the energy $E = -38.90$ cm^{-1}) asymptotic $Br_2(B,v_f < v')$ fragment vibrational state distribution

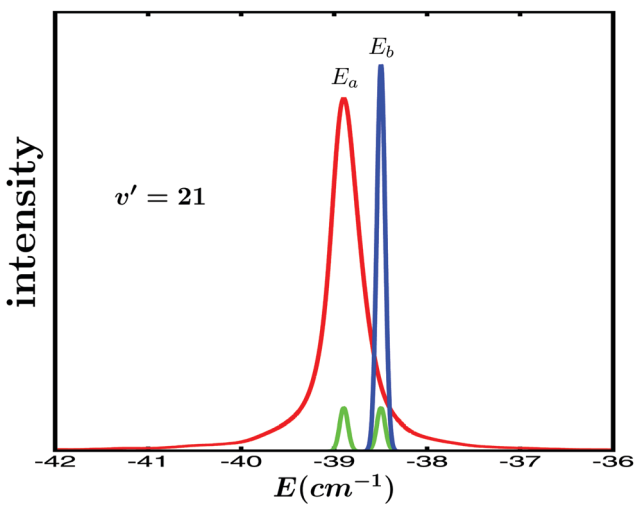

Fig. 1 Lorentzian line shape of the Ne–$Br_2(B,v' = 21, n' = 4)$ intermolecular resonance (red line). The two energies $E_a = -38.9$ cm^{-1} (the resonance energy) and $E_b = -38.5$ cm^{-1} (relative to the Ne + $Br_2(B,v' = 21, j' = 0)$ dissociation threshold) excited by the laser field are indicated in the figure. The spectral profile of the pulses used in the $\varepsilon_l(t)$ (l = 1, 3) fields to excite the E_a and E_b energies (with amplitudes $A_1 = A_2$, green lines, and $A_3 = 3A_1$, blue line) is also shown.

($v_f = v' - 1, v' - 2, v' - 3, \ldots$) produced upon resonance decay. To this purpose, the control strategy adopted is similar to that used with overlapping resonances,[15,35–37] namely to excite two different energies E_a and E_b of the spectrum of Fig. 1 in order to induce interference between them. These two energies are excited by two pulses delayed in time. As previously shown, by varying the delay time between the pulses the interference is controlled, and the enhancement of the resonance lifetime can be optimized.[15,35,36] Modification of the asymptotic fragment distribution only requires a sufficiently long delay time between the pulses, without optimization.

The two energies chosen to induce interference are the resonance energy $E_a = -38.90$ cm^{-1} and $E_b = -38.50$ cm^{-1}, both indicated in Fig. 1. The control scheme applies a pump laser field that combines three Gaussian-shaped pulses with the form

$$\begin{aligned}\varepsilon_3(t) = {} & A_1 e^{-(t-t_1)^2/2\sigma^2} \cos[\omega_1(t - t_1) + \phi_1] \\ & + A_2 e^{-(t-t_2)^2/2\sigma^2} \cos[\omega_2(t - t_2) + \phi_2] \\ & + A_3 e^{-(t-t_3)^2/2\sigma^3} \cos[\omega_2(t - t_3) + \phi_3], \end{aligned} \quad (4)$$

where the first pulse of $\varepsilon_3(t)$, centered at t_1, excites the energy E_a (and a narrow bandwidth around it), with an associated photon frequency ω_1. The two additional pulses centered at t_2 and t_3 excite the second energy E_b (associated with the photon frequency ω_2) that will interfere with E_a. The second pulse of $\varepsilon_3(t)$, delayed by $\Delta t_{12} = t_2 - t_1$ from the first one, is used to induce the interference that makes it possible to enhance the resonance lifetime. The third pulse, delayed by $\Delta t_{13} = t_3 - t_1$ from the first one, allows inducing the interference that modifies the asymptotic $Br_2(B,v_f < v')$ fragment distribution. The combination of three pulses of $\varepsilon_3(t)$ is the simplest laser field that allows control of both the resonance decay lifetime and the fragment state distribution produced.

Regarding the specific parameters used in $\varepsilon_3(t)$ in the simulations, for simplicity it is assumed that $\phi_1 = \phi_2 = \phi_3 = 0$. The amplitudes of the pulses are $A_1 = A_2 = 1.0 \times 10^{-6}$ a.u., and $A_3 = 3A_1$, which correspond to a maximum pulse intensity of about 3.5×10^4 W cm^{-2} and 3.2×10^5 W cm^{-2}, respectively, within the weak-field regime. In practice t_1 is fixed at a value $t_1 = 0$, and t_2 and t_3 are varied. Thus, the delay time between the pulses becomes $\Delta t_{12} = t_2 - t_1 = t_2$ and $\Delta t_{13} = t_3 - t_1 = t_3$. The temporal width of all the pulses (related to σ) is the same, and corresponds to a full width at half maximum of FWHM = 200 ps. The spectral profiles of these pulses are shown in Fig. 1 for the two energies E_a and E_b. They are rather narrow and do not overlap in the energy domain. In addition to the simulations applying the $\varepsilon_3(t)$ field, simulations using a single-pulse field $\varepsilon_1(t) = A_1 e^{-(t-t_1)^2/2\sigma^2} \cos[\omega_1(t - t_1) + \phi_1]$ to excite only the E_a resonance energy were carried out in order to obtain the resonance lifetime and the $Br_2(B,v_f < v')$ distribution in the absence of interference. The same values given above were used for the parameters A_1, t_1, σ, ω_1, and ϕ_1.

Control of the resonance lifetime is achieved by applying the two first pulses of $\varepsilon_3(t)$ with different delay times Δt_{12} in the range -500 ps $\leq \Delta t_{12} \leq 500$ ps. For each value of Δt_{12} the resonance survival probability $I_{n'=4}(t) = |\langle \psi_{n'=4}(t) | \Phi(t) \rangle|^2$ is computed, where $\psi_{n'=4}(t)$ is the resonance wave function and $\Phi(t)$ is the wave packet created by the two first pulses of $\varepsilon_3(t)$. Now the corresponding lifetime, τ, is obtained by fitting $I_{n'=4}(t)$ to the function[38]

$$I_{n'=4}(t_j) = A \int_{-\infty}^{t_j} C(t) [\exp(-(t_j - t)/\tau)] \mathrm{d}t, \quad (5)$$

where $C(t)$ is the cross-correlation function of $\varepsilon_3(t)$ and A is an amplitude scaling parameter.

The $I_{n'=4}(t)$ curves obtained for several values of Δt_{12} are displayed in Fig. 2(a), along with the survival probability computed when only the resonance energy E_a is excited with the single-pulse field $\varepsilon_1(t)$. In Fig. 2(b) a typical fit obtained using eqn (5) is also shown. As expected, the single-energy $I_{n'=4}(t)$ curve displays no structure, since interference is not possible.

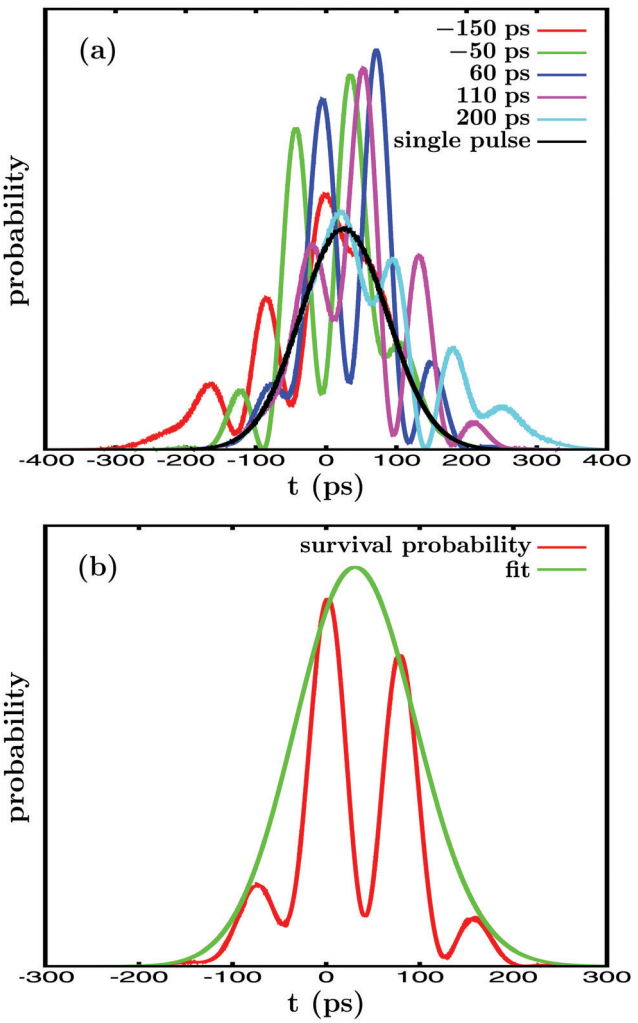

Fig. 2 (a) Resonance survival probability $I_{n'=4}(t)$ computed when $\varepsilon_3(t)$ is applied with different delay times Δt_{12}, from $\Delta t_{12} = -150$ ps to $\Delta t_{12} = 200$ ps, between the pulses exciting the E_a and E_b energies. The corresponding $I_{n'=4}(t)$ curve obtained when the single-pulse field $\varepsilon_1(t)$ is applied to excite only the E_a energy is also displayed. (b) $I_{n'=4}(t)$ curve calculated for the delay time $\Delta t_{12} = 40$ ps (red line), along with the corresponding fit (green line) obtained by using eqn (5).

The lifetime obtained for this curve with eqn (5) is τ_{sing} = 16.0 ps. The two-pulse curves, however, display a pronounced structure of peaks or undulations, which are the signature of quantum interference between the amplitudes excited to the energies E_a and E_b. Actually the different peaks of each curve are separated by the same constant amount of time, which is proportional to the inverse of the energy separation $E_b - E_a$, as expected from an interference event.

Interference between the amplitudes at E_a and E_b requires their simultaneous excitation, and therefore some temporal overlap between the two first pulses of $\varepsilon_3(t)$.[15,36] Thus, the basis of the control scheme applied is the variation of Δt_{12}, because it modifies the temporal overlap between the two first pulses of $\varepsilon_3(t)$. Varying this overlap implies the variation of the relative amplitudes that are excited to both E_a and E_b, and therefore their mechanism of interference. When interference between the amplitudes at E_a and E_b is modified, the shape of the $I_{n'=4}(t)$ curve changes as well, as shown in Fig. 2(a), which leads to the variation of the associated resonance lifetime.

By applying eqn (5) the resonance lifetime is calculated for the different values of Δt_{12}, and the results are plotted in Fig. 3. The figure shows that for very large delay times $|\Delta t_{12}|$ = 500 ps the lifetime found is τ = 16.0 ps, the same value obtained when the single-pulse field $\varepsilon_1(t)$ is applied. For large $|\Delta t_{12}|$ there is no temporal overlap between the two first pulses of $\varepsilon_3(t)$, and thus no interference between E_a and E_b is possible, leading to the same τ obtained with $\varepsilon_1(t)$. However, when $|\Delta t_{12}|$ decreases, the overlap between the pulses becomes nonzero and interference between the amplitudes at E_a and E_b takes place. The result is a gradual enhancement of the resonance lifetime, which increases from τ = 16.0 ps to τ = 31.0 ps at Δt_{12} = 110 ps, nearly twice the value obtained in the absence of interference.

In a previous study[35] the variation of the resonance lifetime was analyzed by changing both the laser fields and the delay times between the pulses, in a framework of overlapping resonances, and such analysis provided very useful insight about how the interference mechanism works. The shape of the curve of Fig. 3 is similar to those found for overlapping resonances,[15,35] indicating that the mechanism of interference operates similarly in the lifetime enhancement. In this sense, the value of Δt_{12} at which maximum lifetime enhancement is achieved is determined by the maximization of the intensity of interference between the amplitudes of E_a and E_b.[35] And the achievement of maximum interference intensity depends on reaching enough temporal overlap between the two pulses (albeit not necessarily the maximum overlap, occurring at Δt_{12} = 0), but such that the mechanism of interference between the amplitudes excited at E_a and E_b is optimized. Such optimization of the interference is what determines the maximum enhancement of the resonance lifetime achieved (τ = 31.0 ps) and the value of Δt_{12} at which it takes place (Δt_{12} = 110 ps in this case).[35,36] It is noted, however, that complete optimization of the laser field (involving going beyond just varying Δt_{12}, and changing the Gaussian shape of the pulses) in order to fully maximize the resonance lifetime enhancement has not been pursued, and thus the enhancement currently achieved could be increased further.

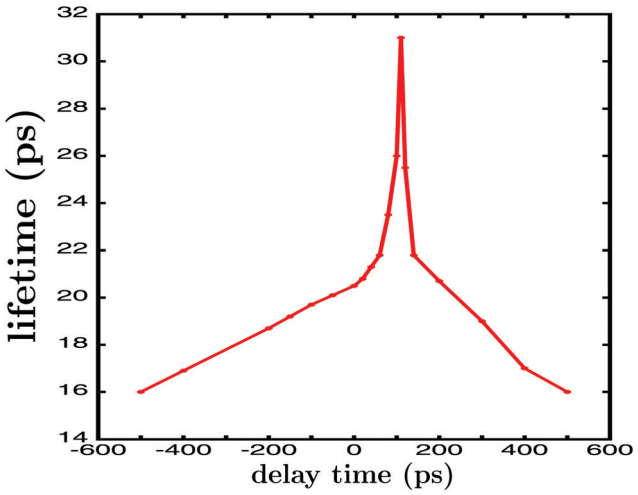

Fig. 3 Lifetime associated with the resonance survival probability $I_{n'=4}(t)$, calculated when the two energies E_a and E_b are excited by the two first pulses of the $\varepsilon_3(t)$ field with different delay times Δt_{12}. The resonance lifetime is significantly enhanced when $|\Delta t_{12}|$ decreases from 500 ps, reaching a maximum enhancement at Δt_{12} = 110 ps.

The next goal is to modify the other resonance properties that determine the outcome of a resonance-mediated molecular process, namely the energy-resolved asymptotic fragment distribution. In the present case it corresponds to the $Br_2(B,v_f < v')$ fragment distribution produced upon predissociation at the resonance energy $E_a = -38.9\ cm^{-1}$. To this end, the third pulse of $\varepsilon_3(t)$ is used to excite the E_b energy, similar to that performed previously with the second pulse. The difference now is that the first and the third pulse will not overlap in time, and the delay time Δt_{13} between them will be much longer than Δt_{12}. The reason for a longer Δt_{13} is to allow enough time for the first amplitude excited at E_a to decay completely and to reach the asymptotic regime of the fragment distribution produced. Thus, by exciting amplitude to E_b, quantum interference is induced between this and the asymptotic decayed amplitude initially excited to E_a by the first pulse of $\varepsilon_3(t)$.[36,37] In the present simulations a long enough delay time Δt_{13} = 1500 ps has been chosen, and in Fig. 4(a) the temporal profile of the $\varepsilon_3(t)$ field applied is displayed, with Δt_{12} = 110 ps, $A_1 = A_2$, and $A_3 = 3A_1$.

In Fig. 4(b) the energy-resolved $Br_2(B,v_f)$ fragment vibrational populations in the $v_f = v' - 1,\ldots,v' - 4$ final vibrational state associated with the E_a resonance energy are shown. The different populations display a clear modification in the asymptotic time regime when the third pulse of $\varepsilon_3(t)$ is applied to excite the E_b energy. Such a modification manifests itself in the form of undulations that reflect the interference taking place between the amplitudes excited at both energies. This interference occurs between the asymptotic amplitude at the E_a energy and the amplitude excited at the E_b energy, which temporarily populates the continuum fragment states at E_a.[36,37] The interference effect is increasingly more intense as the v_f population is larger in magnitude, because the larger is the asymptotic amplitude the more intense will be the interference terms.

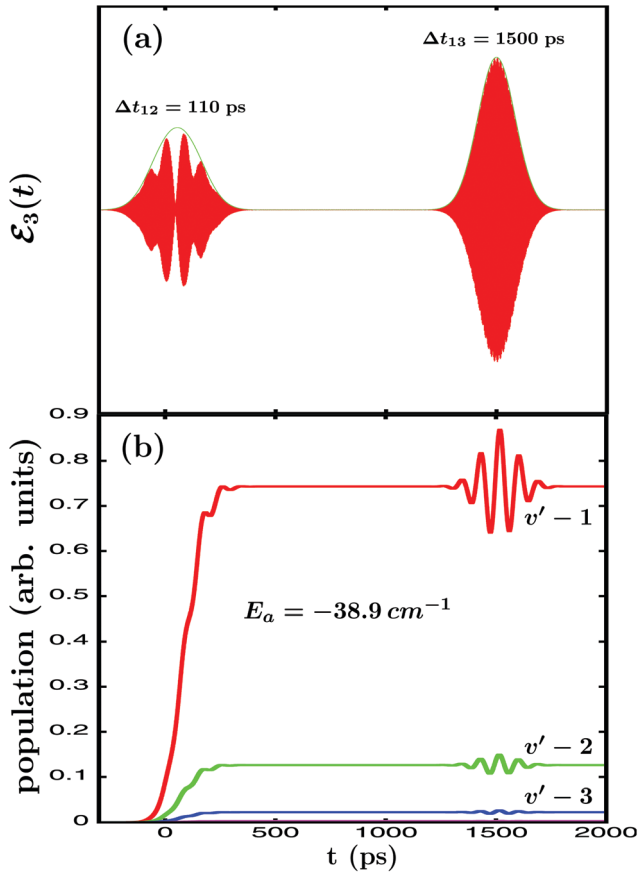

Fig. 4 (a) Temporal profile (red line) along with its envelope (green line) of the $\varepsilon_3(t)$ laser field applied to excite the Ne–$Br_2(B,v' = 21, n' = 4)$ resonance, with Δt_{12} = 110 ps in this case, and Δt_{13} = 1500 ps. (b) Energy-resolved $Br_2(B,v_f)$ fragment vibrational populations in the $v_f = v' - 1,\ldots, v' - 4$ final vibrational state produced upon predissociation of Ne–$Br_2(B,v' = 21, n' = 4)$, associated with the resonance energy $E_a = -38.9$ cm^{-1}, when the $\varepsilon_3(t)$ field of Fig. 4(a) is applied. All the vibrational v_f populations are labeled in the figure except $v_f = v' - 4$, which is very small.

In this sense it is noted that the second pulse of $\varepsilon_3(t)$ also causes an interference effect on the vibrational populations of Fig. 4(b) around Δt_{12} = 110 ps, although being much weaker since $A_2 = A_3/3$. Once the third pulse is over and the amplitude excited at E_b has decayed completely, the asymptotic populations converge back to the values previous to the application of the third pulse. The implication is that the modifications caused by interference in the fragment distribution cannot be observed asymptotically in the same vibronic state ($Br_2(B,v_f)$ in our case) where they are produced. This, however, does not prevent an effective control of the fragment distribution and its observation, if the fragments are detected or moved to other vibronic states of interest (applying a further laser pulse) while the interference effect takes place.

The above results demonstrate numerically that by inducing quantum interference between amplitudes at two different energies by applying a simple laser field like $\varepsilon_3(t)$ of eqn (4), extensive control over the decay lifetime and the asymptotic fragment distribution produced upon decay of an isolated resonance can be achieved in the weak-field regime. In the following the formal theory underlying those results and the present control scheme is developed.

Let $\hat{H}$ be the total Hamiltonian of a general molecular system that supports isolated resonances (Ne–$Br_2(B,v')$ would be an example of such a general system). Following the discussion on the decay of a resonance state of Cohen-Tannoudji *et al.*,[43] we can write $\hat{H}$ as $\hat{H} = \hat{H}_0 + W$, where $\hat{H}_0$ is a zeroth-order Hamiltonian and W is a coupling. The spectrum of $\hat{H}_0$ consists of a set of discrete bound states χ_i (located in the interaction region) with associated energies E_i, and a set of continuum states $\varphi_{E,m}$ (associated with the product fragments in the asymptotic region) with associated energies E, and m being a global label for the fragment internal states. When $W = 0$ the χ_i states are true bound states, but when $W \neq 0$, χ_i become resonances ψ_i that decay to the continuum of $\varphi_{E,m}$ states. These states fulfill the orthogonality relationship

$$\langle\chi_i|\chi_i\rangle = \delta_{ij}, \langle\varphi_{E',m'}|\varphi_{E,m}\rangle = \delta_{m'm}\delta(E' - E), \langle\chi_i|\varphi_{E,m}\rangle = 0, \quad (6)$$

and form a complete basis set in which the state of the system excited at the energy E can be expressed. Let ψ_E be the stationary eigenstates of $\hat{H}$ associated with energy E in the excited electronic state of the molecular system. Such eigenstates (which also form a complete basis set) can be expanded in the set of the χ_i and $\varphi_{E,m}$ states as

$$\psi_E(t) = A_k^{(E)}\chi_k e^{-iE_k t/\hbar} + \sum_{m'}\int dE' B_{E',m'}^{(E)}\varphi_{E',m'}e^{-iE't/\hbar}, \quad (7)$$

where χ_k is the closest discrete state to energy E.

Let us now focus on one of the isolated resonances of our general molecular system. By applying a single-pulse field like $\varepsilon_1(t)$ to excite the resonance energy E_a, a wave packet $\xi_{E_a}(t)$ is created

$$\begin{aligned}\xi_{E_a}(t) &= \int dE'' C_{E''}^{(E_a)}(t)\psi_{E''}(t) = a_k^{(E_a)}(t)\chi_k e^{-iE_k t/\hbar} \\ &\quad + \sum_{m'}\int dE' b_{E',m'}^{(E_a)}(t)\varphi_{E',m'}e^{-iE't/\hbar},\end{aligned} \quad (8)$$

where $a_k^{(E_a)}(t) = \int dE'' C_{E''}^{(E_a)}(t)A_k^{(E'')}$ and $b_{E',m'}^{(E_a)}(t) = \int dE'' C_{E''}^{(E_a)}(t) B_{E',m'}^{(E'')}$. Thus, when two pulses are applied to excite the E_a and E_b energies to induce interference between them, the following wave packet is created

$$\Phi(t) = \xi_{E_a}(t) + \xi_{E_b}(t), \quad (9)$$

with $\xi_{E_a}(t)$ and $\xi_{E_b}(t)$ being the amplitudes excited around E_a and E_b, respectively. It is assumed that the two pulses are spectrally narrow enough such that they, and thus $\xi_{E_a}(t)$ and $\xi_{E_b}(t)$, do not overlap in energy. Now, using eqn (8) we can write,

$$\begin{aligned}\Phi(t) &= \int dE''\left[C_{E''}^{(E_a)}(t) + C_{E''}^{(E_b)}(t)\right]\psi_{E''}(t) \\ &= \left[a_k^{(E_a)}(t) + a_k^{(E_b)}(t)\right]\chi_k e^{-iE_k t/\hbar} \\ &\quad + \sum_{m'}\int dE'\left[b_{E',m'}^{(E_a)}(t) + b_{E',m'}^{(E_b)}(t)\right]\varphi_{E',m'}e^{-iE't/\hbar}.\end{aligned} \quad (10)$$

A resonance wave function ψ_i can also be expressed in terms of the stationary eigenstates ψ_E as

$$\psi_i(t) = \int \mathrm{d}E'' c_{E''}^{(i)} \psi_{E''}(t). \tag{11}$$

Thus, the resonance survival probability $I_i(t)$ is

$$\begin{aligned} I_i(t) &= |\langle \psi_i(t)|\Phi(t)\rangle|^2 \\ &= \left| \int \mathrm{d}E'' \int \mathrm{d}E' c_{E''}^{(i)*} \left[C_{E'}^{(E_\mathrm{a})}(t) + C_{E'}^{(E_\mathrm{b})}(t) \right] \langle \psi_{E''}(t)|\psi_{E'}(t)\rangle \right|^2 \\ &= \left| \int \mathrm{d}E' c_{E'}^{(i)*} \left[C_{E'}^{(E_\mathrm{a})}(t) + C_{E'}^{(E_\mathrm{b})}(t) \right] \right|^2 = \left| d_i^{(E_\mathrm{a})}(t) + d_i^{(E_\mathrm{b})}(t) \right|^2 \\ &= \left| d_i^{(E_\mathrm{a})}(t) \right|^2 + d_i^{(E_\mathrm{a})}(t) d_i^{(E_\mathrm{b})*}(t) + d_i^{(E_\mathrm{a})*}(t) d_i^{(E_\mathrm{b})}(t) + \left| d_i^{(E_\mathrm{b})}(t) \right|^2, \end{aligned} \tag{12}$$

where $\langle \psi_{E''}(t)|\psi_{E'}(t)\rangle = \delta(E'' - E')$, $d_i^{(E_\alpha)}(t) = \int \mathrm{d}E' c_{E'}^{(i)*} C_{E'}^{(E_\alpha)}(t)$, with $\alpha = a,b$.

The term $\left| d_i^{(E_\mathrm{a})}(t) \right|^2$ of eqn (12) is the survival probability that would be obtained if a single resonance energy E_a was excited with the single-pulse field $E_1(t)$ (*i.e.*, the plain curve of Fig. 2(a), with associated lifetime τ_sing = 16.0 ps). The three additional terms of eqn (12) arise from the excitation of amplitude at energy E_b by the second pulse of $\varepsilon_3(t)$, and its interference with the resonance amplitude excited at E_a. Such terms associated with the interference are the ones that cause the undulations of the $I_{n'=4}(t)$ curves of Fig. 2(a). As mentioned above, the requirement for these terms to be nonzero is that the amplitudes $d_i^{(E_\mathrm{a})}(t)$ and $d_i^{(E_\mathrm{b})}(t)$ must be generated simultaneously at E_a and E_b, respectively, which implies the temporal overlap to some extent of the two pulses exciting those energies. When the delay time Δt_{12} between the pulses is varied, the range of temporal overlap between them is modified, changing the relative $d_i^{(E_\mathrm{a})}(t)$ and $d_i^{(E_\mathrm{b})}(t)$ amplitudes excited simultaneously. This causes a variation of the interference terms of eqn (12) in a controlled manner, which leads to a change in the shape of $I_i(t)$ (see Fig. 2(a)), and thus also in the associated lifetime (as shown in Fig. 3). In brief, interference induces a new decay mechanism with a longer lifetime that replaces the intrinsic decay mechanism, in which a transfer of amplitude back and forth between the two energies takes place.[44] Eqn (11) reflects the fact that a resonance state ψ_i possesses a nonzero energy width. This finite width is what makes possible interference of the resonance with itself, when a wave packet $\Phi(t)$ containing different energies within this width (essentially E_a and E_b) is created with the two pulses of the field. This is the key aspect of the present weak-field control scheme of the isolated resonance behavior.

Regarding the fragment state distribution produced upon resonance decay, the asymptotic probability associated with the fragment state $\varphi_{E,m}$ can be expressed as

$$P_m(E, t_\infty) = C \lim_{t\to\infty} \left| \langle \varphi_{E,m}|\Phi(t)\rangle \right|^2 = C \left| \langle \varphi_{E,m}|\Phi(t_\infty)\rangle \right|^2, \tag{13}$$

where C is a constant and $\Phi(t)$ is the wave packet created by the electric field applied. Similarly as with the resonance lifetime, the control strategy here is based on inducing interference by exciting two different energies, namely the resonance energy E_a and the additional energy E_b, with two pulses. Thus a $\Phi(t)$ wave packet like that of eqn (9) and (10) is created. Our goal now is to modify the energy-resolved asymptotic fragment state distribution at the resonance energy E_a, $P_m(E_\mathrm{a},t) = C|\langle \varphi_{Ea,m}|\Phi(t)\rangle|^2$. By using eqn (10) we can write

$$\begin{aligned} \langle \varphi_{E_\mathrm{a},m}|\Phi(t)\rangle &= \sum_{m'} \int \mathrm{d}E' \left[b_{E',m'}^{(E_\mathrm{a})}(t) + b_{E',m'}^{(E_\mathrm{b})}(t) \right] \langle \varphi_{E_\mathrm{a},m}|\varphi_{E',m'}\rangle \mathrm{e}^{-iE't/\hbar} \\ &= \sum_{m'} \int \mathrm{d}E' \left[b_{E',m'}^{(E_\mathrm{a})}(t) + b_{E',m'}^{(E_\mathrm{b})}(t) \right] \delta_{mm'} \delta(E' - E_\mathrm{a}) \mathrm{e}^{-iE't/\hbar} \\ &= \left[b_{E_\mathrm{a},m}^{(E_\mathrm{a})}(t) + b_{E_\mathrm{a},m}^{(E_\mathrm{b})}(t) \right] \mathrm{e}^{-iE_\mathrm{a}t/\hbar}, \end{aligned} \tag{14}$$

where eqn (6) was used. The product state distribution at time t long enough finally becomes

$$\begin{aligned} P_m(E_\mathrm{a}, t) &= C \left| \langle \varphi_{E_\mathrm{a},m}|\Phi(t)\rangle \right|^2 = C \Big[\left| b_{E_\mathrm{a},m}^{(E_\mathrm{a})}(t) \right|^2 + b_{E_\mathrm{a},m}^{(E_\mathrm{a})}(t) b_{E_\mathrm{a},m}^{(E_\mathrm{b})*}(t) \\ &\quad + b_{E_\mathrm{a},m}^{(E_\mathrm{a})*}(t) b_{E_\mathrm{a},m}^{(E_\mathrm{b})}(t) + \left| b_{E_\mathrm{a},m}^{(E_\mathrm{b})}(t) \right|^2 \Big] \end{aligned} \tag{15}$$

Eqn (15) is very similar to eqn (12) because it also consists of a sum of four terms, three of them being the result of excitation of amplitude to the second energy E_b, that generates temporarily the $b_{E_\mathrm{a},m}^{(E_\mathrm{b})}(t)$ amplitude, and its interference with the asymptotic amplitude $b_{E_\mathrm{a},m}^{(E_\mathrm{a})}(t)$ previously excited to E_a. Such interference is what causes the long-time undulations displayed in the vibrational populations of Fig. 4(b). Indeed, the first term of eqn (15), $C\left| b_{E_\mathrm{a},m}^{(E_\mathrm{a})}(t) \right|^2$, is generated when only the E_a energy is excited by the first pulse of $\varepsilon_3(t)$ (or by the single-pulse field $\varepsilon_1(t)$). The three additional terms arising from the excitation to E_b "dress" the first term, producing the interference-induced modification of the fragment distribution in a similar way to the survival probability of eqn (12). The difference with the resonance lifetime control is that now the two pulses are not required to overlap in time, because the amplitude excited to E_a will remain all the time in the continuum fragment states after decay.

The mechanism of interference in this case is the following. After the amplitude excited to E_a has decayed to the continuum fragment states, becoming asymptotic, the third pulse of $\varepsilon_3(t)$ pumps amplitude to the E_b energy. When this latter amplitude decays, it spreads and redistributes temporarily among all the $\varphi_{E,m}$ continuum states accessible by the resonance state within its energy width, including those associated with the E_a energy, $\varphi_{Ea,m}$. This generates temporarily the amplitude $b_{E_\mathrm{a},m}^{(E_\mathrm{b})}(t)$ appearing in the last three terms of eqn (15) that produce the interference effect in the fragment distribution.[36,37] The temporary dispersion of the amplitude excited by the third pulse among different $\varphi_{E,m}$ asymptotic states within a range of energy that includes the $\varphi_{E_\mathrm{a},m}$ fragment states is due to the

uncertainty principle. Once the third pulse of $\varepsilon_3(t)$ is over and all the amplitude excited to E_b has decayed completely to the appropriate $\varphi_{E_b,m}$ fragment states, producing a distribution at energy E_b, interference ceases and the asymptotic distribution at E_a converges again to $P_m(E_a, t_\infty) = C\left|b^{(E_a)}_{E_a,m}(t_\infty)\right|^2$. Since the interference terms of eqn (15) appear as long as the amplitude $\xi_{E_b}(t)$ (or equivalently $b^{(E_b)}_{E_a,m}(t)$) is created by the third pulse of $\varepsilon_3(t)$, it becomes clear that this can be done at any asymptotic time as long as desired, and as many times as desired (using further successive pulses after the third one in the laser field).

The above general equations, and specifically eqn (12) and (15), which govern the resonance survival probability and product fragment distribution, respectively, provide the formal support to the results of the numerical simulations shown in Fig. 2–4. It is stressed that in the derivation of these equations no assumption is made on the nature or type of the molecular system that originates or supports the isolated resonance under control. Therefore these equations are valid for any isolated resonance, regardless of the origin of the system featuring the resonance. The consequence is that the application of the present control scheme behind these equations is general and universal to any molecular system featuring isolated resonance states, thus making possible the control of both the duration and the outcome of any resonance-mediated molecular process.

4 Conclusions

In conclusion, this study demonstrates both numerically and mathematically the possibility to control extensively the dynamical decay behavior of an isolated resonance state, which involves the resonance decay lifetime and the asymptotic fragment state distribution produced upon resonance decay. The weak-field control scheme applied is based on inducing quantum interference between amplitudes excited at two different energies of the resonance line shape, namely the resonance energy and an additional energy. Control is achieved by using a simple laser field consisting of a combination of three pulses with a delay time between them. The first pulse excites the resonance energy, the second pulse excites the second energy in order to control the decay lifetime, and finally the third pulse excites again the second energy at a much longer delay time in order to control the asymptotic fragment distribution. The key aspect of the control scheme is to exploit the property of the resonance state that involves possessing a nonzero energy width, which makes it possible that the resonance state may interfere with itself, and thus allows interference between the amplitudes excited at the two energies of the resonance width used in the scheme. The formal equations developed demonstrate that the application of the scheme is universal to any resonance-mediated molecular process, in order to control both its duration and decay outcome.

Conflicts of interest

There are no conflicts of interest to declare.

Acknowledgements

This work was funded by the Ministerio de Economía y Competitividad (MINECO, Spain), Grants No. CTQ2015-65033-P and PGC2018-096444-B-100. The Centro de Supercomputación de Galicia (CESGA, Spain) is acknowledged for the use of its resources.

References

1 D. Tannor and S. Rice, *J. Chem. Phys.*, 1985, **83**, 5013–5018.
2 P. Brumer and M. Shapiro, *Chem. Phys. Lett.*, 1986, **126**, 541–546.
3 A. Assion, T. Baumert, M. Bergt, T. Brixner, B. Kiefer, V. Seyfried, M. Strehle and G. Gerber, *Science*, 1998, **282**, 919–922.
4 P. Anfinrud, R. de Vivie-Riedle and V. Engel, *Proc. Natl. Acad. Sci. U. S. A.*, 1999, **96**, 8328–8329.
5 S. A. Rice and M. Zhao, *Optical Control of Molecular Dynamics*, Wiley-Interscience, 2000.
6 R. J. Levis, G. M. Menkir and H. Rabitz, *Science*, 2001, **292**, 709–713.
7 E. Skovsen, M. Machholm, T. Ejdrup, J. Thϕgersen and H. Stapelfeldt, *Phys. Rev. Lett.*, 2002, **89**, 133004.
8 C. Daniel, J. Full, L. González, C. Lupulescu, J. Manz, A. Merli, S. Vajda and L. Wöste, *Science*, 2003, **299**, 536–539.
9 M. Shapiro and P. Brumer, *Principles of the Quantum Control of Molecular Processes*, Wiley-Interscience, 2003.
10 B. J. Sussman, D. Townsend, M. I. Ivanov and A. Stolow, *Science*, 2006, **314**, 278–281.
11 G. Katz, M. A. Ratner and R. Kosloff, *Phys. Rev. Lett.*, 2007, **98**, 203006.
12 M. P. A. Branderhorst, P. Londero, P. Wasytcyk, C. Brif, R. L. Kosut, H. Rabitz and I. A. Walmsley, *Science*, 2008, **320**, 638–643.
13 A. B. Henson, S. Gersten, Y. Shagam, J. Narevicius and E. Narevicius, *Science*, 2012, **338**, 234–238.
14 A. García-Vela, *J. Chem. Phys.*, 2012, **136**, 134304.
15 A. García-Vela, *J. Phys. Chem. Lett.*, 2012, **3**, 1941–1945.
16 F. Calegari, *et al.*, *Science*, 2014, **346**, 336–339.
17 M. E. Corrales, J. González-Vázquez, G. Balerdi, I. R. Solá, R. de Nalda and L. Bañares, *Nat. Chem.*, 2014, **6**, 785–790.
18 R. Cireasa, *et al.*, *Nat. Phys.*, 2015, **11**, 654–658.
19 A. Serrano-Jiménez, L. Bañares and A. García-Vela, *Phys. Chem. Chem. Phys.*, 2019, **21**, 7885–7893.
20 R. T. Skodje, D. Skouteris, D. E. Manolopoulos, S. H. Lee, F. Dong and K. Liu, *Phys. Rev. Lett.*, 2000, **85**, 1206–1209.
21 P. S. Chistopher, M. Shapiro and P. Brumer, *J. Chem. Phys.*, 2005, **123**, 064313.
22 M. Qiu, *et al.*, *Science*, 2006, **311**, 1440–1443.
23 D. Gerbasi, A. S. Sanz, P. S. Chistopher, M. Shapiro and P. Brumer, *J. Chem. Phys.*, 2007, **126**, 124307.
24 J. B. Kim, *et al.*, *Science*, 2015, **349**, 510–513.
25 W. Shiu, J. J. Lin and K. Liu, *Phys. Rev. Lett.*, 2004, **92**, 103201–1-4.
26 O. Atabek, R. Lefebvre, M. Lepers, A. Jaouadi, O. Dulieu and V. Kokoouline, *Phys. Rev. Lett.*, 2011, **106**, 173002.
27 S. Chefdeville, *et al.*, *Phys. Rev. Lett.*, 2012, **109**, 023201.

28 T. Westermann, *et al.*, *Angew. Chem., Int. Ed.*, 2014, **53**, 1122–1126.
29 S. N. Vogels, *et al.*, *Science*, 2015, **350**, 787–790.
30 A. García-Vela and N. E. Henriksen, *J. Phys. Chem. Lett.*, 2015, **6**, 824–829.
31 A. Bergeat, J. Onvlee, C. Naulin, A. van der Avoird and M. Costes, *Nat. Chem.*, 2015, **7**, 349–353.
32 C. Naulin and M. Costes, *Chem. Sci.*, 2016, **7**, 2462–2469.
33 A. García-Vela, *Chem. Sci.*, 2017, **8**, 4804–4810.
34 S. Bhattacharyya, S. Mondal and K. Liu, *J. Phys. Chem. Lett.*, 2018, **9**, 5502–5507.
35 A. García-Vela, *Phys. Chem. Chem. Phys.*, 2018, **20**, 3882–3887.
36 A. García-Vela, *Phys. Chem. Chem. Phys.*, 2019, **21**, 7491–7501.
37 A. García-Vela, *Phys. Rev. Lett.*, 2018, **121**, 153204–1-6.
38 J. A. Cabrera, C. R. Bieler, B. C. Olbricht, W. E. van der Veer and K. C. Janda, *J. Chem. Phys.*, 2005, **123**, 054311–1-8.
39 M. A. Taylor, J. M. Pio, W. E. van der Veer and K. C. Janda, *J. Chem. Phys.*, 2010, **132**, 104309.
40 A. García-Vela and K. C. Janda, *J. Chem. Phys.*, 2006, **124**, 034305.
41 A. García-Vela, *J. Chem. Phys.*, 2008, **129**, 094307.
42 A. García-Vela, *Phys. Chem. Chem. Phys.*, 2015, **17**, 29072–29078.
43 C. Cohen-Tannoudji, B. Diu and F. Laloë, *Quantum Mechanics*, John Wiley and Sons, 1977.
44 A. García-Vela, *J. Phys. Chem. A*, 2019, **123**, 7394–7400.